

# In silico Evaluation of Antimicrobial Activity of Some Thiadiazoles Using Molecular Docking Approach †

Amalia Stefaniu <sup>1,\*</sup>, Lucia Pintilie <sup>1</sup>, Veronica Anastasoae <sup>2</sup> and Eleonora-Mihaela Ungureanu <sup>2,\*</sup>

<sup>1</sup> National Institute for Chemical-Pharmaceutical Research and Development, 112 Vitan Av., 031299 Bucharest, Romania; lucia.pintilie@gmail.com

<sup>2</sup> Politehnica University of Bucharest, Gheorghe Polizu 1-7, 011061 Bucharest, Romania; veronyk\_92@yahoo.com

\* Correspondence: astefaniu@gmail.com (A.S.); em\_ungureanu2000@yahoo.com (E.-M.U.)

† Presented at the 24th International Electronic Conference on Synthetic Organic Chemistry, 15 November–15 December 2020; Available online: <https://ecsoc-24.sciforum.net/>.

**Abstract:** Molecular docking studies have been performed to assess the antimicrobial potential of three 1,3,4-thiadiazole derivatives containing azulene rings. The simulations were conducted on *Mycobacterium tuberculosis* DNA gyrase, *Staphylococcus aureus* DNA gyrase, and *Escherichia coli* DNA adenine methylase. The relationships between the structures of compounds and their potential antimicrobial activity were investigated. Interactions with amino acid residues from the active binding site were elucidated and the results of docking are reported in terms of docking score. Better docking scores are obtained for the investigated compounds than for the natural ligand, (4S)-2-methyl-2,4-pentanediol, in the case of the *Mycobacterium tuberculosis*. Two of the studied ligands present better binding affinities against *Escherichia coli* than the co-crystallized ones. Regarding *S. aureus* gyrase, the thiadiazole derivatives exhibit lower docking scores and fewer interactions than the aminobenzimidazole urea inhibitor. Our study can be useful to screen and design similar hybrid active compounds.

**Keywords:** molecular docking; antimicrobial virtual screening; thiadiazoles; azulenes

**Citation:** Stefaniu, A.; Pintilie, L.; Anastasoae, V.; Ungureanu, E.-M. In silico Evaluation of Antimicrobial Activity of Some Thiadiazoles Using Molecular Docking Approach. *Chem. Proc.* **2021**, *3*, 116. <https://doi.org/10.3390/ecsoc-24-08319>

Academic Editors: Julio A. Seijas and M. Pilar Vázquez-Tato

Published: 14 November 2020

**Publisher's Note:** MDPI stays neutral with regard to jurisdictional claims in published maps and institutional affiliations.



**Copyright:** © 2020 by the authors. Licensee MDPI, Basel, Switzerland. This article is an open access article distributed under the terms and conditions of the Creative Commons Attribution (CC BY) license (<http://creativecommons.org/licenses/by/4.0/>).

## 1. Introduction

Heterocyclic compounds, such as thiadiazoles, play an important role among organic compounds possessing pharmacological activity, with potential applications in medicinal chemistry. In literature, some hybrid thiadiazoles-based structures (e.g., 2-phenylamino-5-(4-fluorophenyl)-1,3,4-thiadiazole) are reported as pharmacophore systems, with antituberculosis activity against *Mycobacterium tuberculosis* [1]. 2-Amino-1,3,4-thiadiazole is reported as a promising scaffold to design antimicrobial agents [2].

Starting from such premises, the goal of this study was to examine some hybrid structures containing azulene and thiadiazoles, by computational means as a molecular docking approach to realize a virtual screening for the assessment of their potential biological activity. We chose three different protein targets to evaluate their ability to interact and interfere in the replication process of important and opportunistic pathogens such as *Staphylococcus aureus*, *Mycobacterium tuberculosis*, and *Escherichia coli*. A series of 1,3,4-thiadiazoles, unsubstituted or substituted either at the azulene-1-yl moiety or at the 5-position of the thiadiazole ring were previously synthesized and characterized [3]. By our investigation, we intend to evaluate their possible applications in the field of medicinal chemistry.

## 2. Computational Methodology—Docking Protocol

The docking simulations were carried out using a CLC Drug Discovery Workbench (Qiagen). The protein fragments were imported from the Protein Data Bank: 3M4I: crystal

structure of the second part of the *Mycobacterium tuberculosis* DNA gyrase reaction core: the TOPRIM domain at 1.95 Å resolution, containing the co-crystallized): (4S)-2-methyl-2,4-pentanediol (three-letter code: MPD) [4]; 4P8O: *Staphylococcus aureus* gyrase bound to an aminobenzimidazole urea inhibitor (1-ethyl-3-[5-(5-fluoropyridin-3-yl)-7-(pyrimidin-2-yl)-1H-benzimidazol-2-yl]urea (three-letter code: 883)) [5], and 4RTO: complex of *Escherichia coli* DNA Adenine Methyltransferase (DAM) with Sinefungin and with DNA containing proximal Pap Regulon Sequence [6]. Investigated ligand structures, T1-T3 (see Figure 1a–c) were generated with Spartan 16 Software, Wavefunction Inc, Irvine, USA [7,8], and optimized by energy minimization to prepare \*.sdf files used as input in the docking program. The co-crystallized ligand's pose was validated by redocking and the binding active site was set up. The water molecules and co-factors were removed. Ligands' properties were calculated as well as their accordance with Lipinski's rule of five [9]. The results are given as docking score function and Root Mean Square Deviation (RMSD). Interactions of ligands by hydrogen-bonding with amino acids from the interacting amino acids group of protein fragment's active binding site are depicted and their length was measured.

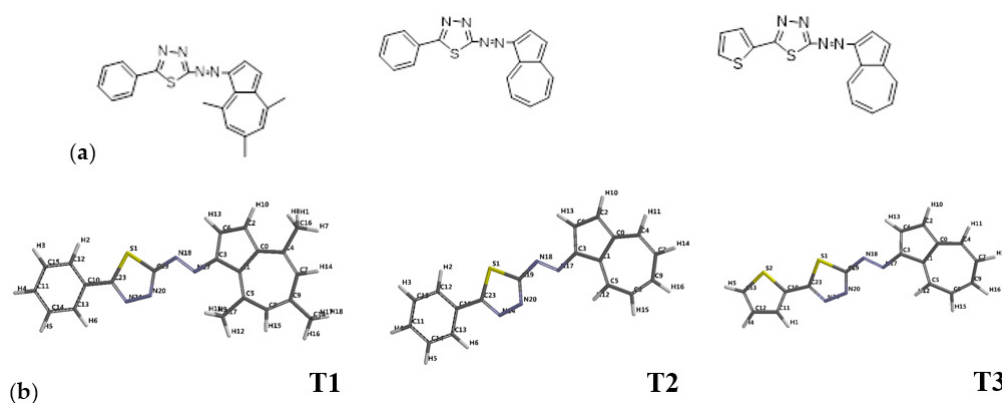


**Figure 1.** 2D structure of T1–T3 thiadiazole derivatives (a) and their 3D optimized structures with atomic numbering labels (b).

### 3. Results and Discussion

Figure 1 illustrates the structure of 1,3,4-thiadiazoles (T1–T3) under investigation, as 2D (a) and optimized 3D structures with atomic labels (b) arbitrarily chosen by Spartan Software.

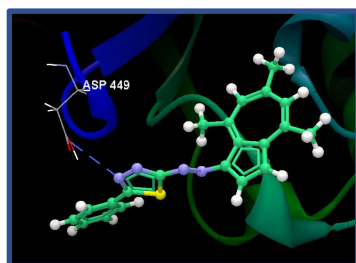
Table 1 lists important molecular descriptors and properties to assess the oral bioavailability according to Lipinski's rule [9], where: MW is the molecular weight, that should be less than 500 Daltons, HBD is the number of hydrogen bond donors, recommended to be lower than 5, HBA is the number of hydrogen bond acceptors with acceptable values less than 10, and the water-octanol partition coefficient (logP) which should be less than 5. The investigated T1–T3 structures reveal one Lipinski's violation, given by the  $\log P > 5$ , thus suggesting their hydrophobic character. These calculations are useful to predict the drug-likeness for drug candidates in virtual screening methodologies. The calculated values of the LogP parameter suggest that all investigated 1,3,4-thiadiazoles are highly lipophilic, with poor aqueous solubility. Generally, values of LogP over 5 suggest poor absorption or permeation. Further optimization of such ligands containing both azulene and thiadiazole moieties, is required in order to increase the hydrophilicity and to favor hydrophilic interactions by means of NH/OH/N/O groups. Thus, the probability to interact with proteins and the ability to become biologically active can be successfully achieved.

Figure 2 reveals the interactions by hydrogen-bonding of T1–T3, with the crystal structure of the second part of the *Mycobacterium tuberculosis* DNA gyrase reaction core:

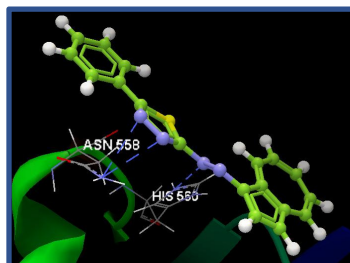
the TOPRIM domain at 1.95 Å resolution. **T2** and **T3** reveal similar scores (43.19 and 40.95, respectively), by forming three hydrogen bonds with the same amino acids residue, with N (sp<sup>2</sup>) HIS560 and N (sp<sup>2</sup>) ASN558, respectively, at the two nitrogen atoms of the thiadiazole aromatic ring, which is commonly known as the structural motif in pharmacology, [10] and one interaction by the diazo bond that links the thiadiazole with the azulene. The planar five-member thiadiazole ring acts as an acceptor in the H-bond formation, in the biological media. Some of the thiadiazole-based structures possess antimicrobial activities, e.g., oxazolidinone analogs possessing 1,3,4-thiadiazole C-ring, designed as hybrids of linezolid [11,12]. Against *Mycobacterium tuberculosis* DNA gyrase, the **T1** compound reveals a lower score than its analogs, **T2** and **T3**, respectively. **T1** forms a single H-bonding with—O (sp<sup>3</sup>) ASP449, as depicted in Table 2.

**Table 1.** Ligands' calculated properties.

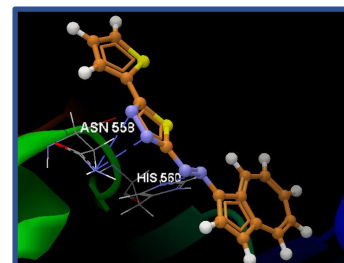
Ligand/ Protein Fragment Source	MW (g·mol <sup>-1</sup> )	HBD	HBA	LogP	Flexible Bonds	Lipinski's Violations
co-crystalized MPDA-1 /3M4I ( <i>M. tuberculosis</i> )	118.17	2	2	0.27	2	0
co-crystalized 883B 301 /4P8O ( <i>S. aureus</i> )	376.37	2	8	1.61	4	0
co-crystalized SFG /4RTO ( <i>E. coli</i> )	382.39	10	12	-3.22	7	2
<b>T1</b>	358.46	0	4	5.24	3	1
<b>T2</b>	326.46	0	4	5.49	3	1
<b>T3</b>	322.41	0	4	5.21	3	1



(a) **T1** H-bonding with ASP449



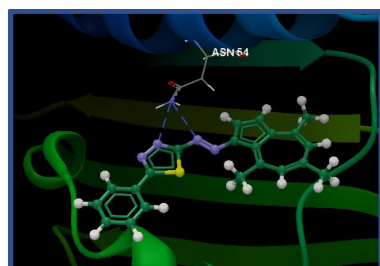
(b) **T2** H-bonding with ASN558 and HIS560



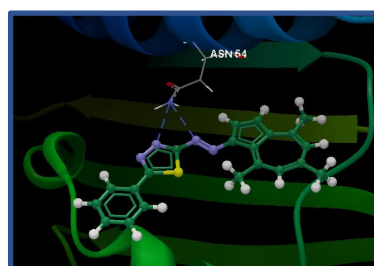
(c) **T3** H-bonding with ASN558 and HIS560

**Figure 2.** **T1–T3** Hydrogen-bonding interactions with amino acid residues from the active binding site of 3M4I (*Mycobacterium tuberculosis* DNA gyrase).

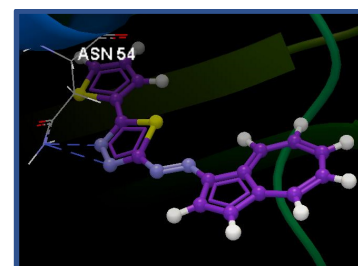
Figure 3 reveals the interactions by Hydrogen-bonding of **T1–T3**, with 4P8O protein fragment from *S. aureus* gyrase.



(a) **T1** H-bonding with ASN54



(b) **T2** H-bonding with ASN54



(c) **T3** H-bonding with ASN54

**Figure 3.** **T1–T3** Hydrogen-bonding interactions with amino acid residues from the active binding site of 4P8O (*S. aureus* gyrase).

**Table 2.** Docking results for 3M4I (*Mycobacterium tuberculosis* DNA gyrase).

Target/Ligand	Interacting Group	Hydrogen Bonds/Length(Å)	Docking Score/RMSD
3M4I/co-crystallized MPDA-1	ARG451, HIS525, PRO450, TYR524, HIS560, GLY520, ILE519, LEU522, ARG523	O4(sp <sup>3</sup> )—O(sp <sup>2</sup> ) LEU522/3.302	−25.91/0.86
3M4I/T1	ASP449, ARG451, PRO450, TYR524, ARG523, LEU522, LYS521, GLY520, ALA508, LEU509, GLY510, THR507	N24(sp <sup>2</sup> )—O(sp <sup>3</sup> ) ASP449/3.247	−38.19/0.06
3M4I/T2	ASN558, HIS560, ILE519, HIS525, ARG451, PRO450, GLY520, TYR524, LEU522, ARG523, LYS521	N18(sp <sup>2</sup> )—N(sp <sup>2</sup> ) HIS560/3.057 N20(sp <sup>2</sup> )—N(sp <sup>2</sup> ) ASN558/3.126 N24(sp <sup>2</sup> )—N(sp <sup>2</sup> ) ASN558/3.103	−43.19/0.69
3M4I/T3	GLU557, ASN558, HIS560, ILE519, HIS525, ARG451, LYS452, ASP449, PRO450, TYR524, GLY520, LEU522, ARG523, LYS521	N17(sp <sup>2</sup> )—N(sp <sup>2</sup> ) HIS560/3.187 N20(sp <sup>2</sup> )—N(sp <sup>2</sup> ) ASN558/2.914 N24(sp <sup>2</sup> )—N(sp <sup>2</sup> ) ASN558/3.135	−40.95/0.72

**Table 3.** Docking results for 4P8O (*Staphylococcus aureus* gyrase).

Target/Ligand	Interacting Group	Hydrogen Bonds/Length(Å)	Docking Score/RMSD
4P8O/co-crystallized	ASN54, VAL52, ILE51, ILE102, VAL79, ILE175, VAL174, THR80, THR173, PRO87, GLY85, ASP81, ARG144, ARG84, GLY83, GLU58, SER55, ILE86	N25(sp <sup>2</sup> )—N(sp <sup>2</sup> ) ARG144/2.769 N6(sp <sup>2</sup> )—O(sp <sup>2</sup> ) ASP81/2.797 N3(sp <sup>2</sup> )—O(sp <sup>2</sup> ) ASP81/2.914 N3(sp <sup>2</sup> )—O(sp <sup>3</sup> ) SER55/3.081	−70.22/0.08
4P8O/T1	SER55, ASN54, GLU58, ASP81, GLY83, GLY172, ARG84, GLY85, ILE86, PRO87, ARG144, ILE102, SER128, THR173	N20(sp <sup>2</sup> )—N(sp <sup>2</sup> ) ASN54/3.062 N18(sp <sup>2</sup> )—N(sp <sup>2</sup> ) ASN54/3.135	−58.08/0.10
4P8O/T2	VAL52, VAL79, ASN54, ILE51, GLU50, SER55, THR80, ASP81, GLU88, GLY83, ARG84, THR173, VAL174, ILE175, GLY85, ARG144, ILE86, PRO87, ILE102	N24(sp <sup>2</sup> )—N(sp <sup>2</sup> ) ASN54/2.790 N20(sp <sup>2</sup> )—N(sp <sup>2</sup> ) ASN54/2.944	−56.49/0.18
4P8O/T3	ASP81, GLU58, GLY83, THR80, SER55, VAL79, ASN54, ILE51, ILE175, VAL174, THR173, ARG84, GLY85, ARG144, ILE86, PRO87, ILE102	N24(sp <sup>2</sup> )—N(sp <sup>2</sup> ) ASN54/2.954 N20(sp <sup>2</sup> )—N(sp <sup>2</sup> ) ASN54/2.903	−53.61/0.19

Table 3 depicts docking results in terms of interactions details, docking score values and interacting group for investigated ligands in relation with *S. aureus*. Regarding docking against the *S. aureus* 4P8O fragment, all 1,3,4-thiadiazoles exhibit lower docking scores than the natural ligand, as shown in Table 3. ASN54 amino acid residue is involved by its

Nsp<sup>2</sup> in two H-bond forming with T1-T3 ligands. Although present in the interacting surrounding group of co-crystallized ligand and thiadiazoles ligands, ASN54 does not interact by hydrogen-bonding with the natural ligand. This compound reveals more interactions (4 H-bonding and a greater docking score). So, lower, maybe inefficient activity of investigated thiadiazoles against *S. aureus* gyrase is expected.

Figure 4 depicts the intramolecular interactions of T1-T3 with 4RTO (*Escherichia coli* DNA Adenine Methyltransferase). Concerning T1 and T2, the thiadiazole ring is involved in H-bonding with different amino acid residues (TRP10 and ASP54, respectively). T3 acts differently, by a nitrogen of the azo bond, that forms a hydrogen bond with ASP54. T1 and T2 reveal greater docking scores than the natural ligand. The obtained score for T3 is lower, as seen in Table 4. The co-crystallized ligand presents interactions within the active binding site, while our investigated thiadiazoles are poorly interacting.

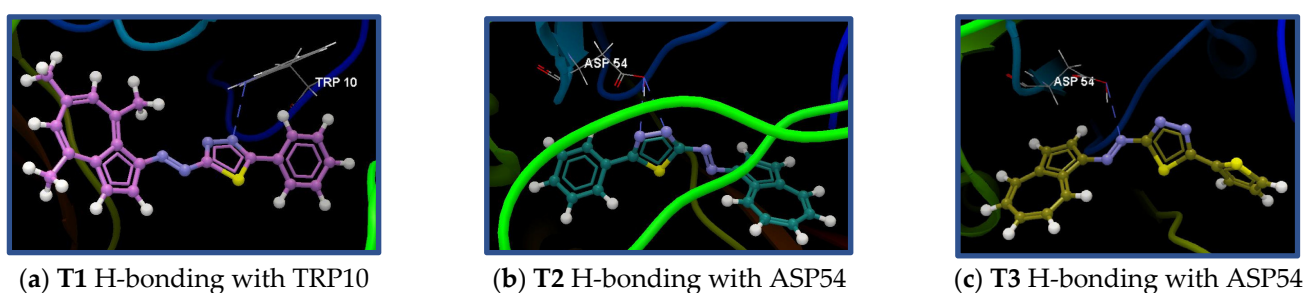


**Figure 4.** T1–T3 Hydrogen-bonding interactions with amino acid residues from the active binding site of 4RTO (*Escherichia coli* DNA Adenine Methyltransferase).

**Table 4.** Docking results for 4RTO (*Escherichia coli* DNA Adenine Methyltransferase).

Target/Ligand	Interacting Group	Hydrogen Bonds/Length (Å)	Docking Score/RMSD
4RTO/co-crystallized SFG	ASN56, ILE55, PHE201, GLU163, SER164, GLN205, TYR165, SER168, LEU59, ASP54, PRO183, PHE35, ALA53, PRO182, PRO34, ASP181, GLU33, TYR179, VAL36, TYR184, VAL41, LYS14, SER40, GLY39, GLY13, GLY12, GLY37, ALA38, ALA11, TRP10	N1 (sp <sup>2</sup> )–N (sp <sup>2</sup> ) TYR165/3.129 O2' (sp <sup>3</sup> )–O (sp <sup>2</sup> ) ASP54/2.654 O3' (sp <sup>3</sup> )–O (sp <sup>3</sup> ) ASP54/2.567 O3' (sp <sup>3</sup> )–N(sp <sup>2</sup> ) TRP10/3.128 O (sp <sup>2</sup> )–N (sp <sup>2</sup> ) ALA38/2.834 OXT (sp <sup>2</sup> )–O (sp <sup>3</sup> ) SER40/2.980 N (sp <sup>3</sup> )–O s(sp <sup>3</sup> ) ASP181/2.426	–67.74/0.79
4RTO/T1	ALA53, VAL36, GLU163, PRO34, ASP54, PHE35, ILE55, SER164, TYR165, ALA166, GLN205, PHE201, SER200, PRO183, ASN120, LEU122, CYS123, ALA11, TRP10, LYS59, ASN115, GLY121	N24 (sp <sup>2</sup> )–N(sp <sup>2</sup> ) TRP10/3.101	–72.21/0.07
4RTO/T2	ALA53, ASP54, GLU163, PRO34, PHE35, ILE55, SER164, TYR165, GLN205, PHE201, TYR184, PRO183, PRO182, ASP181, ALA11, GLY12, TRP10, GLY13	N24 (sp <sup>2</sup> )–O (sp <sup>3</sup> ) ASP54/3.000 N20 (sp <sup>2</sup> )–O (sp <sup>3</sup> ) ASP54/2.982	–71.15/0.07
4RTO/T3	TRP10, ALA11, GLY12, GLY37, VAL36, ASP54, ALA53, ILE55, GLU163, SER164, PHE35, PRO34, TYR165, ASP181, PRO183, PRO182, SER200, TYR184, PHE201, GLN205	N18 (sp <sup>2</sup> )–O (sp <sup>3</sup> ) ASP54/3.304	–66.42/0.23

#### 4. Conclusions

This study opens new opportunities to consider the synthesis and development of new structures derived from thiadiazoles coupled with azulene moieties as possible antimicrobial agents. Further analyses are required in order to establish a possible inhibitory action against pathogens and hybrid structures containing skeletons similar to those used in the present study and must be optimized to acquire high inhibitory activity against pathogenic microorganisms.

#### References

1. Oruç, E.E.; Rollas, S.; Kandemirli, F.; Shvets, N.; Dimoglo, A.S. 1,3,4-Thiadiazole derivatives. synthesis, structure elucidation, and structure–antituberculosis activity relationship investigation. *J. Med. Chem.* **2004**, *47*, 6760–6767, doi:10.1021/jm0495632.
2. Serban, G.; Stanasel, O.; Serban, E.; Bota, S. 2-Amino-1,3,4-thiadiazole as a potential scaffold for promising antimicrobial agents. *Drug Des. Devel. Ther.* **2018**, *12*, 1545–1566, doi:10.2147/DDDT.S155958.
3. Razus, A.; Birzan, L.; Cristea, M.; Tecuceanu, V.; Draghici, C.; Haganu, A.; Maganu, M.; Pintilie, L.; Ungureanu, E.-M., New (azulen-1-ylidiazenyl)-heteroaromatic compounds containing 1,2,5-thiadiazol-3-yl moieties. *Rev. Chim.* **2019**, *70*, 1518–1529.
4. 3M4I Piton, J.; Petrella, S.; Delarue, M.; Andre-Leroux, G.; Jarlier, V.; Aubry, A.; Mayer, C. Structural insights into the quinolone resistance mechanism of Mycobacterium tuberculosis DNA gyrase. *PLoS ONE* **2010**, *5*, e12245.
5. Grillot, A.L.; Tiran, A.L.; Shannon, D.; Krueger, E.; Liao, Y.; O'Dowd, H.; Li, P. Second-generation antibacterial benzimidazole ureas: Discovery of a preclinical candidate with reduced metabolic liability. *J. Med. Chem.* **2014**, *57*, 8792–8816.
6. Horton, J.R.; Zhang, X.; Blumenthal, R.M.; Cheng, X. Structures of Escherichia coli DNA adenine methyltransferase (DAM) in complex with a non-GATC sequence: Potential implications for methylation-independent transcriptional repression. *Nucleic Acids Res.* **2015**, *43*, 4296–4308.
7. Shao, Y.; Molnar, L.F.; Jung, Y.; Kussmann, J.; Ochsenfeld, C.; Brown, S.T.; DiStasio, R.A., Jr. Advances in methods and algorithms in a modern quantum chemistry program package. *Phys. Chem. Chem. Phys.* **2006**, *8*, 3172–3191.
8. Hehre, W.J. *A Guide to Molecular Mechanics and Quantum Chemical Calculations*; Wavefunction, Inc.: Irvine, CA, USA, 2003.
9. Lipinski, C.A. Lead-and drug-like compounds: The rule-of-five revolution. *Drug Discov. Today Technol.* **2004**, *1*, 337–341.
10. Hu, Y.; Li, C.Y.; Wang, X.M.; Yang, Y.H.; Zhu, H.L. 1,3,4-Thiadiazole: Synthesis, reactions, and applications in medicinal, agricultural, and materials chemistry. *Chem. Rev.* **2014**, *114*, 5572–5610.
11. Matysiak, J. Biological and pharmacological activities of 1,3,4-Thiadiazole based compounds. *Mini Reviews Med. Chem.* **2012**, *15*, 762–775.
12. Thomasco, M.; Gadwood, R.C.; Weaver, E.A.; Ochoada, J.M.; Ford, C.W.; Zurenko, G.E.; Hamel, J.C.; Stapert, D.; Moerman, J.K.; Schaadt, R.D.; et al. The synthesis and antibacterial activity of 1,3,4-thiadiazole phenyl oxazolidinone analogues. *Bioorg. Med. Chem. Lett.* **2003**, *13*, 4196–4196.